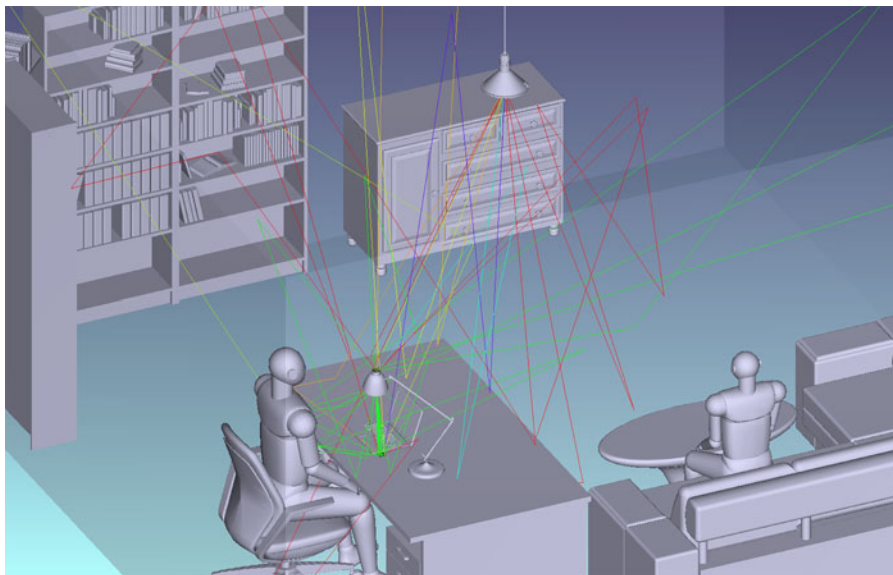# Cooperative Visible Light Communications With Full-Duplex Relaying

Omer Narmanlioglu, *Student Member, IEEE*
Refik Caglar Kizilirmak, *Member, IEEE*
Farshad Miramirkhani, *Student Member, IEEE*
Murat Uysal, *Senior Member, IEEE*

Cooperative Visible Light Communications With Full-Duplex Relaying

Omer Narmanlioglu,[1] *Student Member, IEEE,*
Refik Caglar Kizilirmak,[2] *Member, IEEE,*
Farshad Miramirkhani,[1] *Student Member, IEEE,*
and Murat Uysal,[1] *Senior Member, IEEE*

[1]Department of Electrical and Electronics Engineering, Ozyegin University, Istanbul 34794, Turkey
[2]Department of Electrical and Electronics Engineering, Nazarbayev University, Astana 0100000, Kazakhstan

Abstract: In this paper, we investigate cooperative visible light communication (VLC) system where an intermediate light source acts as a relay terminal. We assume that relay terminal operates in full-duplex mode. In contrast to radio frequency counterparts, full-duplex VLC terminal is relatively easier to implement due to directive propagation characteristic of light. We first model VLC relay terminal taking into account loop interference channel based on ray tracing simulations. Then, we investigate error rate performance of the relay-assisted VLC system. Our performance evaluations demonstrate the superiority of full-duplex relaying over half-duplex counterpart especially for high modulation sizes.

Index Terms: Visible light communication, relay-assisted communication, full-duplex relaying.

1. Introduction

Visible light communication (VLC), also known as LiFi, refers to the dual use of light emitting diodes (LEDs) for both illumination and communication purposes. LEDs can be modulated at very high speeds that are not noticeable to human eye. This lets the use of LEDs as ubiquitous wireless access points. As a powerful alternative and/or complementary radio-frequency (RF) solutions, VLC has been receiving a growing attention from academic and industrial circles [1], [2].

In some indoor environments, there exist multiple luminaries. In addition to ceiling ambient lights, there can be secondary light sources such as desk or floor lights used for task lighting purposes. This motivates the deployment of such secondary light sources as relaying terminals to boost the link reliability and/or extend coverage [3]–[5]. Similarly, ceiling lights can act as relay terminals for each other in a multi-hop fashion. Either half-duplex (HD) or full-duplex (FD) relaying can be employed. In the context of RF communication, HD relaying is typically preferred. This necessitates from the fact that transmit and receive power levels differ from each other by orders of magnitude. In an FD RF relay terminal, the strong locally transmitted signal will couple the receiver and hence overwhelm

the far weaker received signal. The coupling signal is often referred to as loop interference [6]. In contrary to RF, FD relaying is relatively easier to implement in VLC systems since loop interference is expected to be at lower levels due to more directive illumination pattern of light source. There have been some earlier attempts on the investigation of FD relaying in the context of VLC systems. Particularly, the works in [4] and [5] consider relaying scenarios where ceiling lights arranged in linear and triangular topologies help each other through multi-hop transmission. The underlying channel models therein are however oversimplified; only the line-of-sight (LOS) component between the transmitter and receiver is considered and multipath components are ignored. Furthermore, these works are based on the assumption of single-carrier architecture and use simple pulse modulation techniques.

VLC channel is of multipath nature and targeting data rates on the order of multiple Gbits/sec over a multipath channel with typical delay spreads of nanoseconds requires to deal with severe inter-symbol-interference (ISI) [7]. This can be mitigated either through the use of time-domain equalization in single-carrier systems or multi-carrier communication techniques, particularly in the form of orthogonal frequency division multiplexing (OFDM). The powerful combination of relay-assisted transmission and OFDM has been first investigated in [8], later in [9]. Based on the use of HD relaying, it has been shown that significant performance gains can be obtained via cooperation compared to direct transmission. Those gains however vanish, as the modulation size gets larger, due to the fact that HD relaying uses additional time slots for relaying phase, effectively decreasing spectral efficiency. FD relaying has the potential to improve the spectral efficiency, but, to the best of our knowledge, has not yet been explored in multi-carrier VLC systems.

To fill this research gap, we investigate an OFDM-based VLC system with FD relaying. We first develop a realistic indoor VLC channel model and present the channel impulse response (CIR) for loop interference channel, i.e., from relay transmitter to relay receiver. Based on this channel model, we evaluate the bit error rate (BER) performance of OFDM VLC systems with FD relaying and compare its performance with both direct transmission (i.e., no relaying) and HD relaying. Our results reveal that FD relaying significantly outperforms HD relaying and becomes the obvious choice for high modulation orders.

The remainder of the paper is organized as follows. In Section 2, we describe the full duplex VLC relay model with loop interference. In Section 3, we present our overall system model. In Section 4, we present analytical BER calculations followed by numerical results in Section 5. We finally conclude in Section 6.

Notation: $(.)^*$, $[.]^T$ and $\otimes$ respectively denote complex conjugation, transpose and linear convolution operations. $\delta(t)$ is the impulse function, and erfc(.) is the complementary Gauss error function. $x(t) \overset{FT}{\leftrightarrow} X(f) = \int x(t)e^{-j2\pi ft}dt$ and $x[n] \overset{DFT}{\leftrightarrow} X[k] = \sum_{n=0}^{N-1} x[n]e^{-j2\pi nk/N}$ for $n, k \in \{0, 1, ..., N-1\}$ denote continuous Fourier transform (FT) and $N-$point discrete Fourier transform (DFT), respectively.

2. Full Duplex VLC Relaying Terminal Model With Loop Interference

The IEEE has established the standardization group 802.15.7r1 "Short Range Optical Wireless Communications" which is currently in the process of developing a standard for VLC. As a part of ongoing standardization work, reference channel models were proposed by the IEEE 802.15.7r1 Task Group for evaluation of VLC system proposals. These were developed for typical indoor environments including home, office and manufacturing cells [2], [10], [11]. One specific scenario, Scenario 2 of [2], is useful for the performance evaluation of relay-assisted VLC systems where an office room with two light sources, is considered and optical CIRs for source-to-destination (S→D), source-to-relay (S→R), and relay-to-destination (R→D) are presented. Furthermore, the channel modeling methodology adopted in [2] incorporates the presence of objects (e.g., furniture, human body, etc) and wavelength-dependent reflection characteristics of surface materials (e.g., ceilings, floor, walls, furniture, clothes of human beings, etc). It should be however noted that a loop interference channel model (i.e., relay transmitter to relay receiver) is not available within [2].
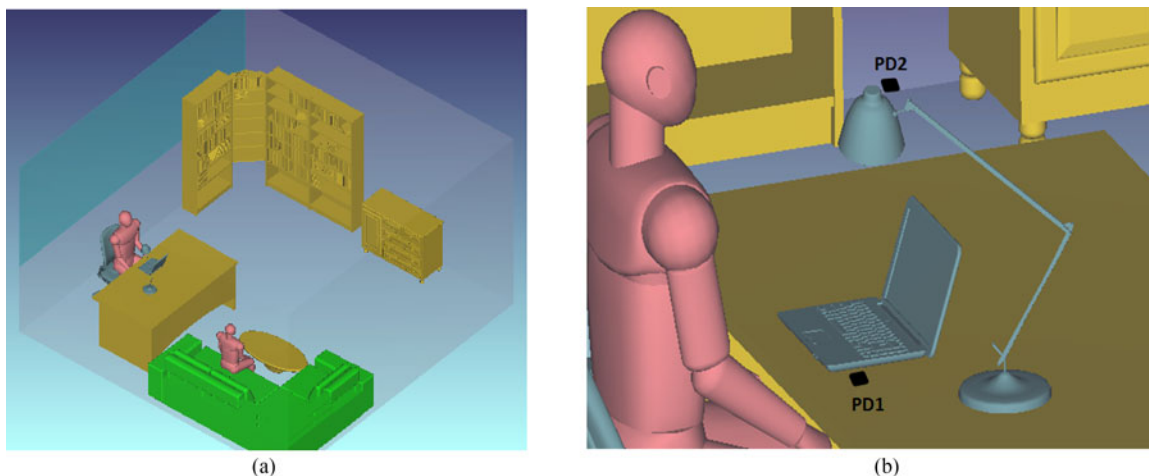
Fig. 1. Indoor office room with secondary light and (b) enlarged version of (a) showing secondary light, i.e., desklight.

TABLE 1
Indoor Office Room Specifications [10]

Luminary Specifications	Brand: LR24-38SKA35 Cree Inc. Half viewing angle: 40°
Photodetector	Field-of-view: 85° Surface area: 1 cm^2
Specifications of Objects and Surfaces	Walls: Plaster
	Ceiling: Plaster
	Floor: Pinewood
	Desk: Pinewood
	Desklight: Black gloss paint
	Library: Pinewood
	Couch: Cotton
	Coffee table: Pinewood
	Shoes: Black gloss paint
	Head & Hands: Absorbing
	Clothes: Cotton
	Laptop: Black gloss paint

Here, we consider the same specifications of Scenario 2 [2] and obtain the CIR associated with loop interference channel. As illustrated in Fig. 1(a), an office room with dimensions of 5 m × 5 m × 3 m is considered. The ceiling light is connected to the data backbone and serves as the source terminal. The desk light has no access to the data backbone and serves as the relay terminal. The destination terminal is connected to a laptop which is placed on the desk. The receiver unit of the destination terminal is on the desk next to the laptop, see PD1 in Fig. 1(b). This might, for example, take the form of a USB-type device connected to laptop. The receiver unit of the relay terminal is on the top of desk light with 45° rotation towards the source on the ceiling, see PD2 in Fig. 1(b). Other specifications considered in the simulation are summarized in Table 1.
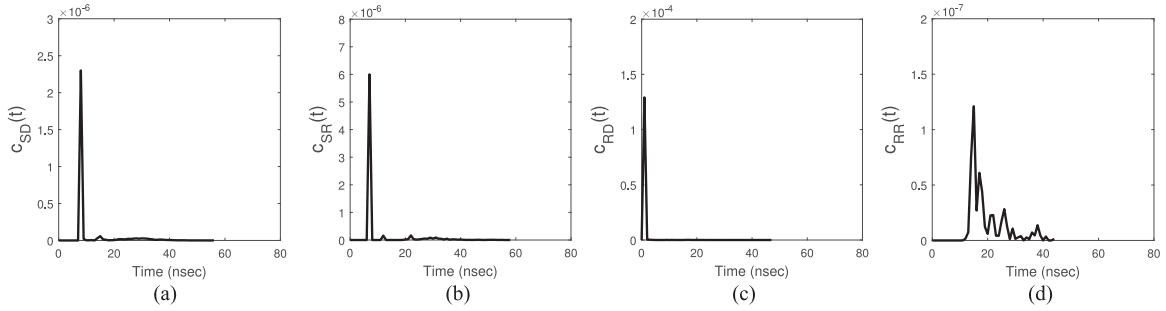
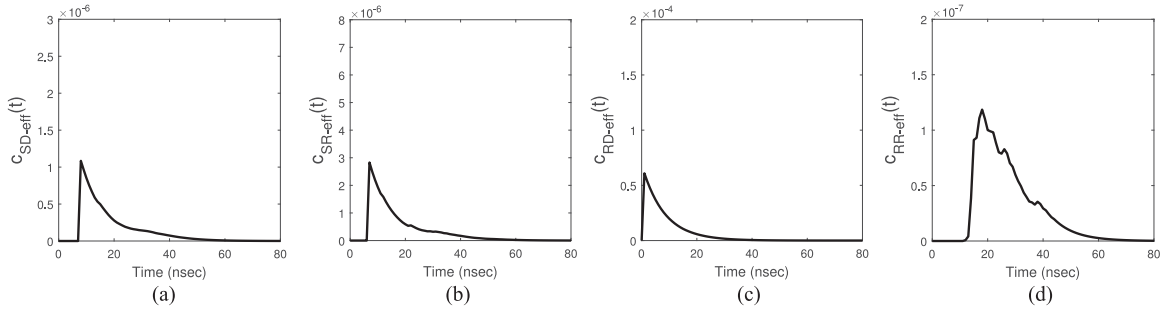Fig. 2. Optical CIRs of (a) S→D, (b) S→R, (c) R→D and (d) R→R channels.

Fig. 3. Effective CIRs of (a) S→D, (b) S→R, (c) R→D and (d) R→R channels.

Optical CIRs for S→D, S→R and R→D, i.e., $c_{SD}(t)$, $c_{SR}(t)$ and $c_{RD}(t)$, can be found in [11] and presented in Fig. 2 for the completeness of presentation. Adopting the channel modelling approach in [7] based on non-sequential ray tracing, we obtain the CIR for loop interference channel, i.e., from desk light's LED to its own photodetector (PD). This is denoted as $c_{RR}(t)$ and presented as Fig. 2(d). It is observed that the delay spread of loop interference channel (R→R) is higher than those in S→D, S→R, and R→D channels while its power level is significantly lower. Mathematically speaking, the DC gains of S→D, S→R, and R→D channels are respectively 2.82×10^{-6}, 7.14×10^{-6}, and 1.31×10^{-4}. This reduces to 5.26×10^{-7} for the R→R channel.

In addition to the multipath propagation environment, the low-pass filter characteristics of LED sources should be further considered. The frequency response of LED is assumed to be [12]

$$C_{LED}(f) = \frac{1}{1 + j\frac{f}{f_{\text{cut-off}}}} \tag{1}$$

where $f_{\text{cut-off}}$ is the LED 3-dB cut-off frequency. The effective CIRs that take into account both multipath propagation and the LED characteristics can be then expressed as $c_{SD-\text{eff}}(t) = c_{SD}(t) \otimes c_{LED}(t)$, $c_{SR-\text{eff}}(t) = c_{SR}(t) \otimes c_{LED}(t)$, $c_{RD-\text{eff}}(t) = c_{RD}(t) \otimes c_{LED}(t)$ and $c_{RR-\text{eff}}(t) = c_{RR}(t) \otimes c_{LED}(t)$ where $c_{LED}(t) \overset{FT}{\leftrightarrow} C_{LED}(f)$. Assume $f_{\text{cut-off}} = 20$ MHz. The corresponding effective CIRs are provided in Fig. 3. It is observed that LED characteristics are the major source for frequency-selectivity.

Inspired from the interference model developed in [13] for RF systems, the mathematical model of an FD VLC relay terminal with the use of amplify-and-forward (AF) relaying is depicted in Fig. 4. In FD relay-assisted transmission under consideration, the relay terminal receives the information from the source and forwards it to the destination after amplification/scaling process (with G_A denoting the amplification gain). An amount of processing delay (denoted as T_P) is introduced as a result of optical-to-electrical conversion, electrical-to-optical conversion and amplification in the terminal. The loop interference channel acts as a feedback link in this model.
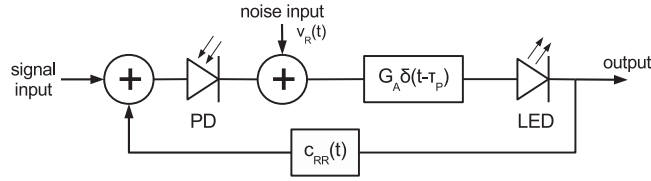
Fig. 4. Mathematical model of FD VLC relay terminal.

Let P denote the total electrical power budget (i.e., shared by source and relay terminals). The optimization parameter K_P defines the fraction of the total electrical information power to be shared between the source and relay terminals. The average transmitted powers from the source and the relay are then respectively defined as $P_{S,TX} = PK_P$ and $P_{R,TX} = P(1 - K_P)$. The average power of received signal at the relay terminal can be written as

$$P_{R,RX} = P_{S,TX} r^2 \int \left| c_{SR-eff}(t) \right|^2 + P_{R,TX} r^2 \int \left| c_{RR-eff}(t) \right|^2 + \sigma_V^2, \tag{2}$$

where r is the responsivity of PD and $V_R(t)$ denotes the additive white Gaussian noise (AWGN) term with zero mean and variance of σ_V^2. The first term in (2) represents the power of received signal from source terminal while the second term corresponds to the power of received signal due to loop interference.

The impulse responses of the FD relay terminal separately for signal and noise inputs (see Fig. 4) are given by

$$h_{R,signal}(t) = G_A \left(r\delta(t - T_p) \otimes c_{LED}(t) + r\delta(t - T_p) \otimes h_{R,signal}(t) \otimes c_{RR-eff}(t) \right), \tag{3}$$

$$h_{R,noise}(t) = G_A \left(\delta(t - T_p) \otimes c_{LED}(t) + r\delta(t - T_p) \otimes h_{R,noise}(t) \otimes c_{RR-eff}(t) \right), \tag{4}$$

where $G_A = \sqrt{\frac{P_{R,TX}}{P_{R,RX}}}$. As a result of the positive feedback due to the $c_{RR-eff}(t)$, the impulse responses given by (3) and (4) have infinite length. In practice, they decay to negligible values and can be truncated.

3. System Model

Our system model builds upon direct current biased optical OFDM (DCO-OFDM). At the source terminal, the bit streams are first mapped to complex-valued modulation symbols $s_1\ s_2\ ...\ s_{N/2-1}$, where N is the number of subcarriers. Phase shift keying (PSK) or quadrature amplitude modulation (QAM) can be used as modulation schemes. To ensure that the output of inverse DFT (IDFT) is real-valued, Hermitian symmetry is imposed which yields

$$\mathbf{X} = \begin{bmatrix} 0\ s_1\ s_2\ ...\ s_{N/2-1}\ 0\ s_{N/2-1}^*\ ...\ s_2^*\ s_1^* \end{bmatrix}^\mathsf{T}. \tag{5}$$

The output of IDFT can be written as

$$x[n] = \frac{1}{\sqrt{N}} \sum_{k=0}^{N-1} X[k] e^{j\frac{2\pi nk}{N}}, \quad n \in \{0, 1, ..., N - 1\}, \tag{6}$$

where $X[k]$ is the kth element of $\mathbf{X}$. Let $\tilde{x}[n]$, $n = 0, 1, ..., N + N_{CP} - 1$ denote the resulting signal after the cyclic prefix (CP) with a length of N_{CP} is appended. Hence, the continuous time domain waveform that drives the LED is given by

$$x_S(t) = \left\{ \sum_{n=0}^{N+N_{CP}-1} \tilde{x}[n]\delta(t - nT_S) \right\} \otimes g_T(t) + B_{DC}, \tag{7}$$

where $g_T(t)$ is the transmit pulse shape filter and B_{DC} is the DC bias voltage which is added to shift the signal into dynamic range of LED [14], [15].

The emitted signal from the source terminal propagates through S→D and S→R→D channels and arrives at the destination. Based on (3) and (4), the end-to-end CIRs that include both S→D and S→R→D links can be written for the information signal and the noise respectively as

$$\tilde{h}_{\text{signal}}(t) = c_{\text{SD-eff}}(t) + c_{\text{SR-eff}}(t) \otimes h_{\text{R,signal}}(t) \otimes c_{\text{RD}}(t), \tag{8}$$

$$\tilde{h}_{\text{noise}}(t) = h_{\text{R,noise}}(t) \otimes c_{\text{RD}}(t). \tag{9}$$

Let $g_R(t)$ denote the receive pulse shape filter matched to $g_T(t)$. After matched filtering, the received electrical signal at the destination is written as

$$y_D(t) = \left(\sqrt{PK_P} r x_S(t) \otimes \tilde{h}_{\text{signal}}(t) + r v_R(t) \otimes \tilde{h}_{\text{noise}}(t) + v_D(t) \right) \otimes g_R(t) \tag{10}$$

where $v_D(t)$ is AWGN term with zero mean and variance of σ_V^2. Let $h_{\text{signal}}[n]$ denote the sampled version of $h_{\text{signal}}(t) = g_T(t) \otimes \tilde{h}_{\text{signal}}(t) \otimes g_R(t)$ which can be expressed as

$$h_{\text{signal}}[n] = h_{\text{signal}}(t)|_{t=nT_s+\tau_0}, \tag{11}$$

where τ_0 is the offset term introduced for synchronization purposes. In practice, it can be calculated as

$$\tau_0 = \arg\max_{\tau} \left[\sum_{n=-\infty}^{\infty} \left| h_{\text{signal}}(nT_S + \tau) \right|^2 \right]. \tag{12}$$

The corresponding frequency domain signal at the kth subcarrier is then given by

$$Y_D[k] = \sqrt{PK_P} r X_S[k] H_{\text{signal}}[k] + r V_R[k] H_{\text{noise}}[k] + V_D[k] G_R[k] \tag{13}$$

where $h_{\text{signal}}[n] \overset{DFT}{\leftrightarrow} H_{\text{signal}}[k]$, $v_R[n] \overset{DFT}{\leftrightarrow} V_R[k]$, $v_D[n] \overset{DFT}{\leftrightarrow} V_D[k]$, $g_R[n] \overset{DFT}{\leftrightarrow} G_R[k]$ and $h_{\text{noise}}[n] \overset{DFT}{\leftrightarrow} H_{\text{noise}}[k]$. The decision is based on the Maximum Likelihood (ML) rule which can be written as

$$\hat{X}[k] = \arg\min_{X \in \Psi} \left[\left\| Y_D[k] - \sqrt{PK_P} r H_{\text{signal}}[k] X \right\|^2 \right], \tag{14}$$

where Ψ denotes the constellation points of deployed modulation.

4. BER Performance

Average BER for an OFDM system can be calculated by

$$\text{BER} = \frac{2}{N-2} \sum_{k=1}^{N/2-1} \text{BER}_{\text{SC}}[k]. \tag{15}$$

In (15), $\text{BER}_{\text{SC}}[k]$ denotes BER per subcarrier as a function of signal-to-noise (SNR) and can be calculated by [16]

$$\text{BER}_{\text{SC}}[k] \approx \begin{cases} \frac{1}{2}\text{erfc}\left(\sqrt{\text{SNR}[k]}\right) & , \quad 2-\text{PSK} \\ \frac{(\sqrt{M}-1)}{\sqrt{M}\log_2\sqrt{M}}\text{erfc}\left(\sqrt{\frac{3\text{SNR}[k]}{(2(M-1))}}\right) & , \quad \text{square } M-\text{QAM} \\ \frac{1}{\log_2(U \times J)}\left[\frac{U-1}{U}\text{erfc}\left(\sqrt{\frac{3\text{SNR}[k]}{U^2+J^2-2}}\right) + \frac{J-1}{J}\text{erfc}\left(\sqrt{\frac{3\text{SNR}[k]}{U^2+J^2-2}}\right)\right] & , \quad \text{rectangular } U \times J-\text{QAM} \end{cases} \tag{16}$$

TABLE 2

Optimum K_P Values

Avg. Signal Power (P)	K_P	Avg. Signal Power (P)	K_P
0 dBm	0.8019	10 dBm	0.9306
1 dBm	0.8118	11 dBm	0.9306
2 dBm	0.8316	12 dBm	0.9405
3 dBm	0.8415	13 dBm	0.9504
4 dBm	0.8613	14 dBm	0.9504
5 dBm	0.8712	15 dBm	0.9603
6 dBm	0.8811	16 dBm	0.9702
7 dBm	0.8910	17 dBm	0.9702
8 dBm	0.9108	18 dBm	0.9702
9 dBm	0.9207	19 dBm	0.9801

Based on (14), SNR per subcarrier can be written as

$$\text{SNR}_\text{FD}[k] = \frac{PK_P r^2 \left|H_\text{signal}[k]\right|^2}{\sigma_V^2 \left(|G_R[k]|^2 + |rH_\text{noise}[k]G_R[k]|^2\right)}. \tag{17}$$

As benchmarks, we also consider the performance of direct transmission and HD relaying. The associated SNRs can be written as [8]

$$\text{SNR}_\text{Direct}[k] = \frac{Pr^2 |H_\text{SD}[k]|^2}{\sigma_V^2 |G_R[k]|^2}, \tag{18}$$

$$\text{SNR}_\text{HD}[k] = \frac{2PK_P r^2 |H_\text{SD}[k]|^2}{\sigma_V^2 |G_R[k]|^2} + \frac{2PK_P r^4 G_A^2 |H_\text{SR}[k]H_\text{RD}[k]|^2}{\sigma_V^2 \left(|G_R[k]|^2 + |rG_A C_\text{RD}[k]G_R[k]|^2\right)}. \tag{19}$$

The BER performance can be further improved through the proper choice of K_P, i.e., optimal power allocation between the terminals. K_P controls the fraction of the total electrical information energy (i.e., AC energy) to be shared between the source and relay terminals. This allocation does not affect the brightness level of the terminals since the average amplitude of the information waveforms in both terminals is still B_{DC} [17].

Due to the negative exponential dependency, minimization of the BER per subcarrier becomes equivalent to the maximization of SNR in (17). In order to minimize BER given by (15), we conduct brute-force search and obtain K_P values provided in Table 2. It is observed that the optimum K_P is 0.8019 for $P = 0$ dBm. In other words, about 80% of the AC power should be allocated to the source terminal while the relay terminal consumes approximately 20% of the total power for BER optimization. For $P = 10$ dBm, the optimum value of K_P becomes 0.9306, indicating that the source terminal should now consume about 93% of the total AC power budget.

5. Numerical Results

In this section, we present the BER performance of the FD relaying and compare it with direct transmission and HD relaying under both optimum power allocation (OPA) and equal power allocation (EPA). In EPA, total available power is shared equally between the source and relay terminals, i.e.,

TABLE 3
Simulation Parameters

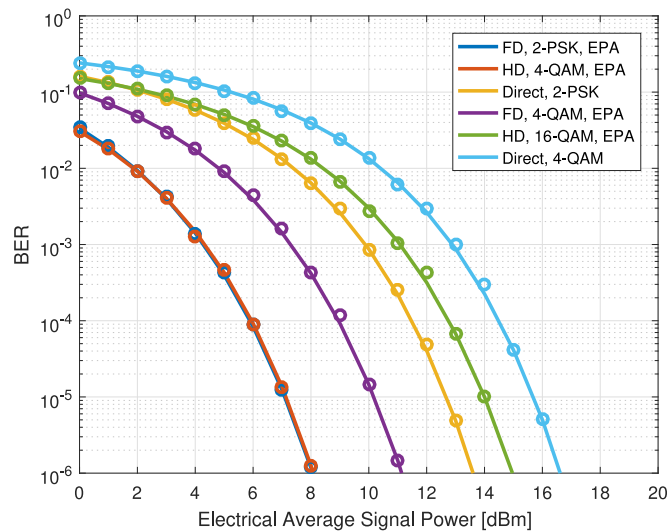|	
Number of subcarriers (N)	256
Cyclic prefix length (N_{CP})	32
Sampling interval (T_S)	250 nsec
Photodetector responsivity (r)	0.28 A/W [18]
Process delay (T_P)	50 nsec
Pulse shaping filters ($g_T(t)$ and $g_R(t)$)	Square root raised cosine filter with roll-off factor of 0.5
Noise power spectral density	10^{-20} W/Hz

Fig. 5. BER performance of relay-assisted and direct transmissions for throughput rates of 1 and 2 bits/sec/Hz.

$K_P = 0.5$. In OPA, optimized values of K_P in Table 2 are used. The CIRs used in the simulation study are already presented in Fig. 3. Other system parameters are given in Table 3.

As discussed in Section 2, the impulse responses of the FD relay terminal for signal and noise terms, given by (3) and (4), have infinite length as a result of the positive feedback. However, the impact of the loop channel degrades drastically and we truncate (3) and (4) where the gains drop 100 dB below their peak values.

In Fig. 5, 2-PSK is used for both direct and FD relaying. In order to maintain an equal throughput for a fair comparison, 4-QAM is used for HD relaying that requires two phase transmission. Therefore, all three schemes achieve a throughput of 1 bit/sec/Hz. EPA is assumed, i.e., $K_P = 0.5$. It is observed from Fig. 5 that HD relaying slightly outperforms FD relaying while both relaying techniques significantly outperform direct transmission. In Fig. 5, we also include the performance of relaying schemes that achieve a throughput rate of 2 bits/sec/Hz, i.e., 4-QAM and 16-QAM respectively for FD and HD relaying. It is observed that when the modulation size increases, FD relaying is able to outperform HD counterpart. Specifically, at a BER of 10^{-3}, a performance improvement of 3.9 dB is obtained. It is also observed that the performance gain over direct transmission is 5.7 dB. Monte-Carlo simulation results are further included in these figures (shown by markers) and provide a perfect match with theoretical BER results.
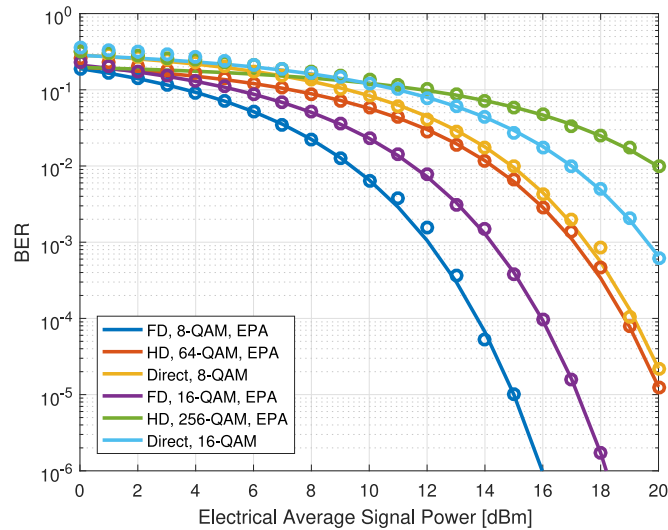
Fig. 6. BER performance of relay-assisted and direct transmissions for throughput rates of 3 and 4 bits/sec/Hz.
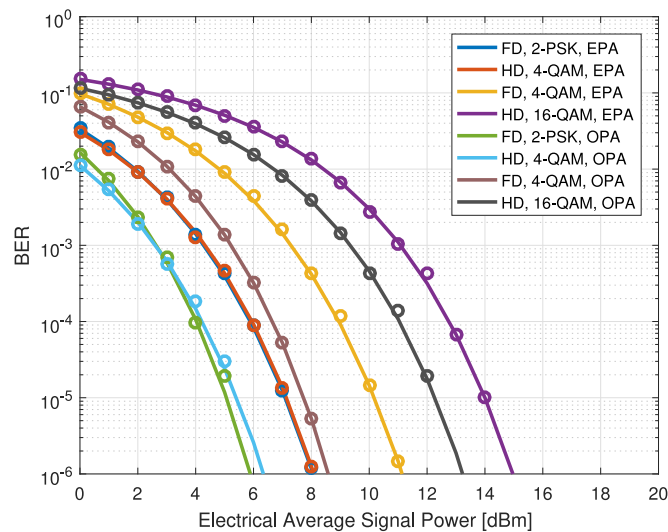

Fig. 7. BER performance of relay-assisted transmissions with EPA and OPA at throughput rates of 1 and 2 bits/sec/Hz.

Benefits of FD relaying over HD relaying become more obvious with the further increase in modulation sizes. In Fig. 6, EPA is assumed and throughput rates of 3 and 4 bits/sec/Hz are targeted. 8-QAM and 16-QAM are used for FD relaying while 64-QAM and 256-QAM are used for HD relaying, respectively. It is observed that the improvement of HD relaying over direct transmission is negligible while FD relaying is able to outperform direct transmission with a gain of 5.7 dB at the throughput rate of 3 bits/sec/Hz. Finally, when a throughput rate of 4 bit/sec/Hz is considered, it is observed that HD relaying performs worse than the direct transmission whereas FD relaying maintains the same gain.

In Fig. 7, we illustrate the improvement in BER performance through OPA. At the throughput of 1 bit/sec/Hz, the performance gain in HD relaying with OPA over EPA is 1.7 dB. This gain remains the same for the throughput of 2 bits/sec. It is observed that FD relaying benefits more from OPA.
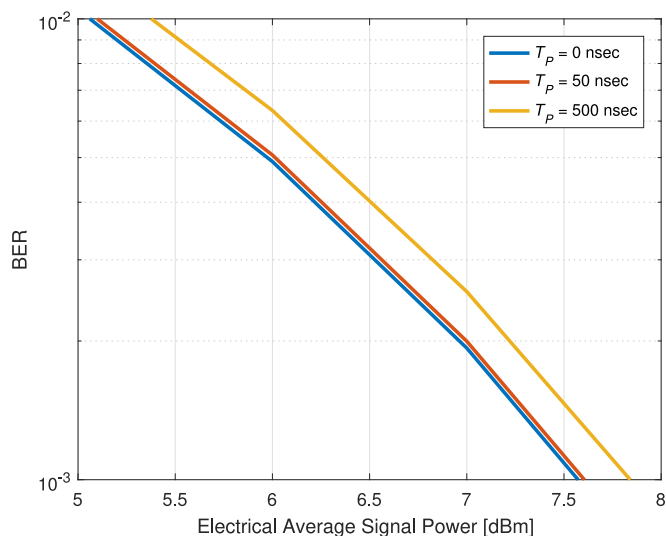
Fig. 8. BER performance for different process delays in FD relaying.

Performance improvements through OPA are 1.7 dB and 2.2 dB respectively at throughput of 1 bit/sec/Hz and 2 bits/sec/Hz.

In the previous simulation results, we set the process delay (T_P) as 50 nsec. In the following, we investigate how processing delay at HD relay terminal affects the overall performance. 4-QAM is deployed. As observed from Fig. 8, the best performance result is obviously achieved when there is no processing delay at the relay terminal (i.e., $T_P = 0$). This is because the signals received from source and relay terminals overlap and boost the total received power at the destination terminal as a consequence of minimization of channel delay spread caused by the FD relays. When a delay with an amount of 50 nsec is introduced, a very slight performance degradation (around 0.01 dB) is observed. This increases to approximately 0.3 dB for 500 nsec process delay.

6. Conclusion

In this work, we have investigated the performance of FD relaying in VLC systems. First, we have proposed a loop interference channel using ray tracing simulations. Due to the relatively directive propagation characteristic of light, the loop interference is found to be low which allows implementation of FD relaying in practice for VLC systems without any additional complexity. Our performance evaluations have clearly demonstrated the superiority of FD relaying over HD counterpart particularly for large modulation sizes. For smaller modulation sizes, HD relaying slightly outperforms FD relaying while both relaying techniques significantly outperform direct transmission. As the modulation size gets larger, the improvement of HD relaying over direct transmission is negligible while FD relaying significantly outperforms direct transmission. For the modulation sizes under consideration, performance gains up to 5.7 dB are observed for HD relaying. We have also shown that additional performance improvements are possible through optimal power allocation among source and relay terminals.

References

[1] D. Karunatilaka, F. Zafar, V. Kalavally, and R. Parthiban, "LED based indoor visible light communications: State of the art," *IEEE Commun. Surveys Tutorials*, vol. 17, no. 3, pp. 1649–1678, Jul.–Sep. 2015.
[2] M. Uysal, F. Miramirkhani, O. Narmanlioglu, T. Baykas, and E. Panayirci, "IEEE 802.15.7r1 reference channel models for visible light communications," *IEEE Commun. Mag.*, vol. 55, no. 1, pp. 212–217, Jan. 2017.

[3] S. Vikramaditya, T. A. Sewaiwar, and Y. H. Chung, "An efficient repeater assisted visible light communication", in *Proc. 21th Eur. Wireless Conf.*, May 2015, pp. 1–5.

[4] H. Yang and A. Pandharipande, "Full-duplex relay VLC in LED lighting linear system topology," in *Proc. 39th Annu. Conf. IEEE Ind. Electron. Soc.*, Nov. 2013, pp. 6075–6080.

[5] H. Yang and A. Pandharipande, "Full-Duplex relay VLC in LED lighting triangular system topology," *in Proc. 6th Int. Symp. Commun., Control Signal Process.*, May 2014, pp. 85–88.

[6] T. Riihonen, S. Werner, and R. Wichman, "Hybrid full-duplex/half-duplex relaying with transmit power adaptation," *IEEE Trans. Wireless Commun.*, vol. 10, no. 9, pp. 3074–3085, Sep. 2011.

[7] F. Miramirkhani and M. Uysal, "Channel modeling and characterization for visible light communications," *IEEE Photon. J.*, vol. 7, no. 6, pp. 1–16, Dec. 2015.

[8] R. C. Kizilirmak, O. Narmanlioglu, and M. Uysal, "Relay-assisted OFDM-based visible light communications," *IEEE Trans. Commun.*, vol. 63, no. 10, pp. 3765–3778, Oct. 2015.

[9] H. Kazemi and H. Haas, "Downlink cooperation with fractional frequency reuse in DCO-OFDMA optical attocell networks," *Proc. IEEE Int. Conf. Commun.*, Kuala Lumpur, Malaysia, 2016, pp. 1–6.

[10] M. Uysal, F. Miramirkhani, T. Baykas, N. Serafimovski, and V. Jungnickel, "LiFi channel models: office, home and manufacturing cell," doc: IEEE 802.15-15/0685r0, Sep. 2015. [Online]. Available: https://mentor.ieee.org/802.15/dcn/15/15-0685-00-007a-lifi-reference-channel-models-office-home-manufacturing-cell.pdf

[11] M. Uysal, T. Baykas, F. Miramirkhani, N. Serafimovski, and V. Jungnickel, "TG7r1 channel model document for high-rate PD communications," doc: IEEE 802.15-15/0746r1, Sep. 2015. [Online]. Avail-able: https://mentor.ieee.org/802.15/dcn/15/15-15-0746-01-007a-tg7r1-channel-model-document-for-high-rate-pd-communications.pdf

[12] L. Grobe and K. D. Langer, "Block-Based PAM with frequency domain equalization in visible light communications," in *Proc. IEEE Globecom Workshops (GC Wkshps)*, 2013, pp. 1070–1075.

[13] G. J. Gonzalez, F. H. Gregorio, J. Cousseau, T. Riihonen and R. Wichman, "Performance analysis of full-duplex AF relaying with transceiver hardware impairments," in *Proc. 22th Eur. Wireless Conf.*, Oulu, Finland, 2016, pp. 1–5.

[14] J. Armstrong, "OFDM for optical communications," *IEEE J. Lightw. Technol.*, vol. 27, no. 3, pp. 189–204, Feb. 2009.

[15] R. Mesleh, H. Elgala, and H. Haas, "On the performance of different OFDM based optical wireless communication systems," *J. Opt. Commun. Netw.*, vol. 3, no. 8, pp. 620–628, 2011.

[16] K. Cho and D. Yoon, "On the general BER expression of one-and two-dimensional amplitude modulations," *IEEE Trans. Commun.*, vol. 50, no. 7, pp. 1074–1080, Jul. 2002.

[17] T. D. C. Little and H. Elgala, "Adaptation of OFDM under visible light communications and illumination constraints," in *Proc. 2014 48th Asilomar Conf. Signals, Syst. Comput.*, 2014, pp. 1739–1744.

[18] J. Grubor *et al.*, "Broadband information broadcasting using LED-Based interior lighting," *IEEE J. Lightw. Technol.*, vol. 26, no. 24, pp. 3883–3892, Dec. 2008.